

# **Micro-Rockets**

**12/06/02**

ME 381 MEMS  
Professor H. Espinosa  
Northwestern University

Nik Hrabe  
Albert Hung  
Josh Mehling  
Arno Merkle

## **Project Summary**

In the area of jet propulsion, micro-scale rockets offer the possibility of attaining increased thrust-to-weight ratios as compared to conventional large rockets. Coupled with the ease of fabrication, such devices open up a wide range of applications in the realm of small payload delivery and guidance systems. The three different designs currently being explored include turbine engine, gaseous propellant, and solid propellant rockets. The first part of the paper gives a general overview of each design and possible applications, outlining their respective advantages and disadvantages which include wear properties, friction, efficiency, robustness, fuel energy densities, and fabrication processes. This is followed by an in-depth case study of the solid propellant rocket, touching on design parameters, step-by-step fabrication techniques, and materials considerations. The results and future direction of current research are discussed for this solid propellant design and the micro-scale rocket field as a whole.

# Table of Contents

## **Introduction**

<b>Microrocket Comparisons</b> .....	5
<i>Turbine engine</i> .....	6
<i>Gaseous Propellant Rocket</i> .....	8
<i>Solid Propellant Rocket</i> .....	9

## **Case Study: Solid Propellant Rocket**

<b>Fabrication</b> .....	10
<i>Convergent/Microheater</i> .....	11
<i>Propellant Chamber</i> .....	13
<i>Divergent</i> .....	16
<i>Assembly of Components</i> .....	16
<b>Materials Considerations</b> .....	17
<i>Propellant Chamber</i> .....	17
<i>Solid Propellant</i> .....	18
<b>Geometric Considerations</b> .....	19
<i>Model</i> .....	19
<i>Chamber-to-Throat Area Ratio</i> .....	19
<i>Divergent</i> .....	20

<b><u>Conclusion</u></b> .....	21
--------------------------------	----

<b><u>Appendix</u></b> .....	22
------------------------------	----

<b><u>References</u></b> .....	28
--------------------------------	----

<b><u>About the Authors</u></b> .....	29
---------------------------------------	----

## List of Figures and Tables

Figure 1: Micro-turbine layout and operation

Figure 2: Gaseous-propelled liquid-cooled micro-rocket

Figure 3: Array of solid propellants micro-rockets

Figure 4: Schematic of Rossi micro-rocket

Figure 5: Schematic of a micro-heater

Figure 6: Array of micro-heaters

Figure 7: Single micro-heater

Figure 8: Propellant chambers

Figure 9: Cross-sectioned propellant chamber

Figure 10: Fuel-filling machine

Table 1: Properties of Si and Macor<sup>®</sup>

Table 2: Chamber-to-Throat ratio results

## **Introduction**

Microelectromechanical Systems (MEMS) is a field of research that, in its short lifetime, has contributed several significant advances in a variety of scientific and technological applications. In miniaturizing mechanical and electronic systems, one can achieve unique responses from materials in ways that benefit performance and efficiency. Innovations requiring miniaturization have resulted in the advancement of microelectronic chip designs, pressure and chemical sensing devices, accelerometers, communications devices, and biologically applicable devices, to name a few. Scaling devices to a microscale allows surface interactions to dominate behavior, creating increased sensitivity in some sensing applications. Approaches to microfabrication, whereby MEMS devices are manufactured, have undergone plentiful examination and optimization, allowing for accurate tolerances and design freedom on the microscale.

This report will analyze one application of such MEMS devices: the microrocket. This device deals almost entirely in the mechanical regime of MEMS devices, most simply existing as a scaled-down version of common macro-scale rockets. Dimensions of such devices are on the order of millimeters, with parts extending to tens of microns, depending on the particular design. Motivations for creating these millimeter-sized rockets include mobility for attached MEMS sensing devices (Smart Dust[1]), guidance systems, and efficiency. Advances in microfabrication allow us to manipulate materials including semiconductors, metals and ceramics. Naturally, materials considerations are paramount in establishing adequate and reliable performance. Ceramics, in particular, are of interest in microrocket applications due to their structural stability under extreme thermal operating environments.

An investigation into the current state of microrocket design, application and fabrication is presented in this paper. Three classes of rockets are summarized (gas turbine, gaseous propellant, and solid propellant), highlighting their respective advantages and disadvantages in performance and fabrication. Following this, a comprehensive investigation into the microfabrication of the solid propellant microrocket is presented.

## Micro-Rocket Comparisons

### *Turbine Engine*

The first type of micro-rocket, and the most widely researched to date, is the microfabricated high-speed gas turbine. This system, which is modeled after its more common “macro-scale” counterparts, can be used in a wide range of applications including cooling, compression, heat engines, and propulsion. While the micro-gas turbine’s use as a source of propulsion is limited in most applications to micro-airplanes rather than micro-rockets, both the design and the fabrication process provide important advances to the current state of the art in micro-scale propulsion.

Turbine engines are about 2cm square with a depth anywhere between 3 and 4mm

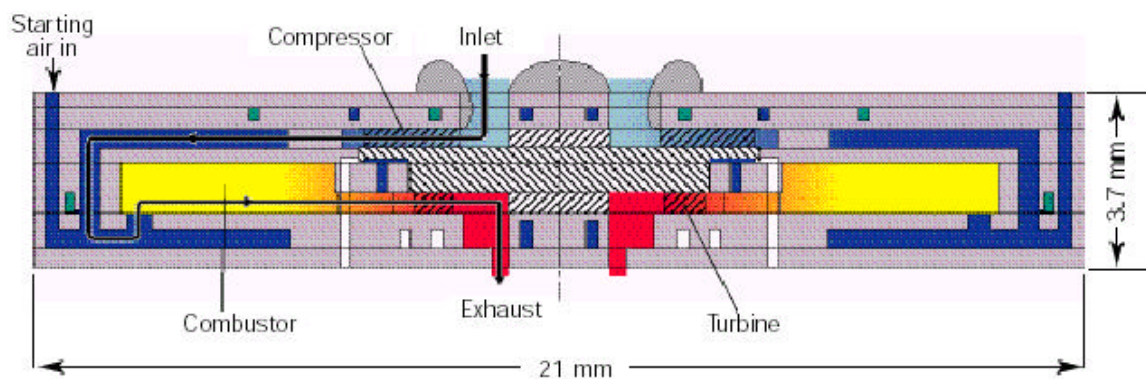


Figure 1: Micro-Turbine Layout and Operation [2]

and their main feature is a rotating disk, 8mm in diameter, mounted along a shaft in the middle of the system [2]. The disk is driven by feeding an air/fuel mixture into a chamber surrounding the disk then igniting this mixture to drive the turbine and exhaust the resulting pressurized gas (See Figure 1). Because of the complex geometry and relative motion of the components the microfabrication steps to build the micro-turbine engine are quite complicated. Six individual silicon wafers are etched using deep reactive ion etching (DRIE) and then wafer bonded together. This stack-up, which can be seen in Figure 1, makes alignment accuracy a concern during fabrication. Because the pressurized exhaust, and thus the propulsion, is created by the rotating turbine, the speed at which the disk spins in relation to the shaft is also of critical importance to the efficiency of the system. To have a comparable power density to macro-scale turbines used in large-scale propulsion, like airplane engines, micro-turbines must rotate with a rotor tip speed of about 500 m/s, or at approximately 1,200,000 rpm [3]. While this has been achieved, most notably by Fréchette, et al at MIT, there are problems in efficiency that arise from this high power density. As larger speeds are reached, energetic losses and the chance of failure increase due to frictional forces. In fact the development of novel, micro-bearings to increase the average 20% efficiency that micro-turbines get is a major focus of current research. While the uses and benefits of micro-turbine engines are clearly there, the problems associated with downscaling rapidly moving parts has been the major stumbling block in fully realizing micro-turbine powered micro-rockets.

### *Gaseous Propellant Rocket*

In an effort to overcome the problems associated with frictional losses and moving parts, some research is being directed towards micro-rockets designed with no moving parts. These designs, one of which is a gaseous propelled, liquid cooled rocket, are expected to be used in future spacecraft and small micro-satellites because of their reusability and the long service

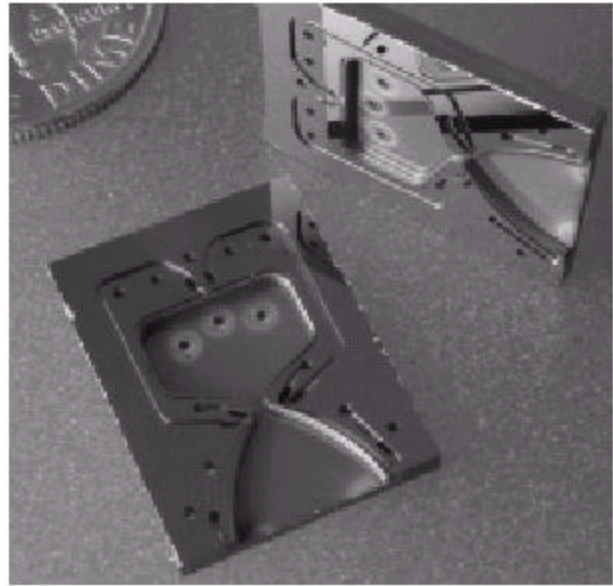


Figure 2: Gaseous Propelled, Liquid Cooled Micro-Rocket [5]

life associated with no moving features [4]. The rocket is made from 6 single crystal silicon wafers, each approximately 4" square. To allow for the high aspect ratio features seen in Figure 2, deep reactive ion etching (DRIE) is used in conjunction with more standard chemical vapor deposition (CVD) and buffered oxide etching (BOE) techniques to fabricate the micro-rocket. Unlike the micro-turbine, this rocket gains all of its thrust force from careful design of the chamber and nozzle geometry. Thus, 3-dimensional contours must be created using largely 2-dimensional fabrication techniques, creating a challenging and relatively slow process requiring as many as 18 anisotropic dry etches and 10 photolithographic chrome masks [4]. The difficulties in fabrication are more than made up for in the success of the device, however. Recent tests on the first generation liquid cooled, gaseous propelled micro-rocket were largely successful. The device created a full Newton in thrust with a useful thrust power of 750 W [4]. The resulting 85:1 thrust to weight ratio, while still lower than desirable, was a product of small

internal chamber pressures. With future tests planned to increase the chamber pressure by an order of magnitude, experimenters expect that the gaseous propelled rocket will eventually yield up to a 1000:1 thrust to weight ratio.

### *Solid Propellant Rocket*

While the micro-turbine and the gaseous propelled rocket are both steps forward in micropropulsion, they both have disadvantages, namely a difficult fabrication procedure and the need for a bulky external system to provide the liquid and gaseous fuel components. Solutions to these problems have been explored in the third type of micro-rocket engine, the solid propellant rocket.

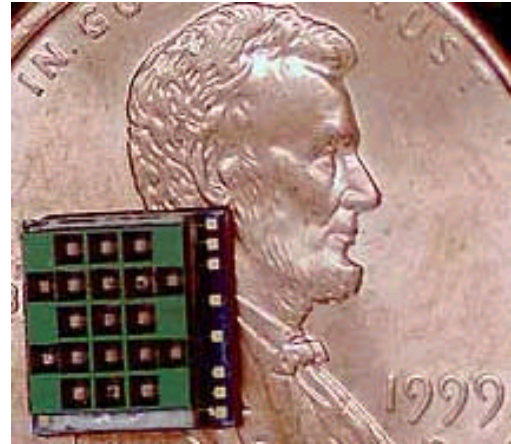


Figure 3: An Array of Solid Propellant Micro-Rockets [7]

This design has a lower total thrust force than the gaseous propelled rocket (4 mN to 1 N), but it is smaller and also has the ability to provide a greater energy density than commercial batteries and other small power sources [6]. The solid propellant rocket design also has the advantage of being easier to fabricate and customizable in regards to fuel selection. The main limitation of this type of device as explained by Rossi et al, is the lack of restart ability [6]. But even this problem is overcome by fabricating large arrays of rockets and using a digital control scheme to control the firing. The size of the solid propellant combustion chamber and nozzle make assembling arrays feasible because even these groups remain quite small in overall dimensions (See Figure 3).

The specific design and current performance progress of the solid propellant rocket is of particular interest because it is this micro-rocket type that offers the greatest opportunity for advancements in micro-satellite and other future small spacecraft propulsion. The solid propellant rocket is relatively easy to fabricate with simple techniques such as anisotropic etching and the fuel source is both customizable and, for the most part, self-contained. These advantages as well as its high energy density make this design the natural choice for space-based applications. Thus, to fully explore the cutting edge of micro-rocket research, an in depth case study will follow which focuses on the specific attributes of the solid propellant micro-rocket. The design's step-by-step fabrication techniques and geometric and materials considerations will be examined in an effort to fully realize the extent to which this design has revolutionized both micro-propulsion and the use of micro-rockets.

## **Case Study: Solid Propellant Microrocket**

### **Fabrication**

To explore some of the fabrication methods utilized in microrockets, the solid propellant design of C. Rossi, et al.[6] will be discussed in detail (see Figure 4 for a schematic of their design and terminology of components). As might be noticed, the schematic in Figure 4, depicts the dimensions of the microrocket components with cylindrical shapes, when in actuality, all components, due to anisotropic etching constraints, are limited to rectangular and pyramidal shapes. It is important to note, that the fabrication technique presented by C. Rossi, et al., is lacking certain details that can be filled in using inferences from the procedure and other sources pertinent to the topic.

The fabrication of this design can be broken down by its components: a convergent/microheater (See steps 1-12 in Appendix A), propellant chamber (steps 13-16), and divergent (steps 17-22). The assembly of these components (steps 23-24) is also a part of fabrication.

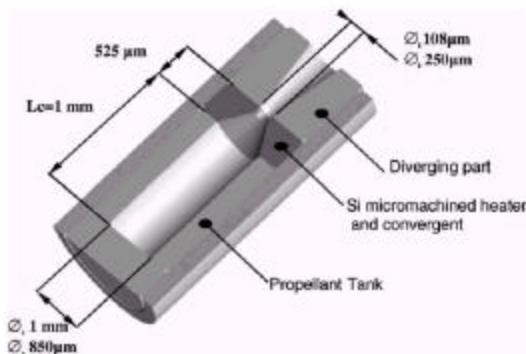


Figure 4: Schematic of Rossi microrocket design including component nomenclature [6]

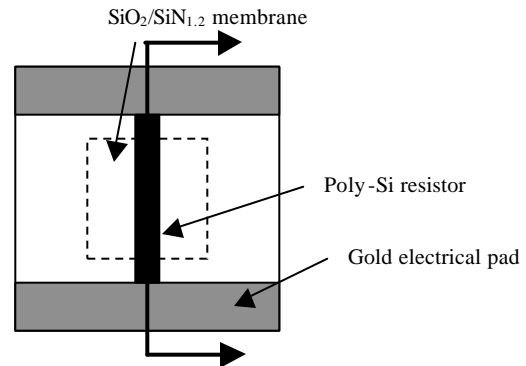


Figure 5: Schematic of a microheater [8] and representation of cross-section seen in process flow diagram (Appendix A)

### *Convergent/Microheater*

The microheater consists of a thin dielectric membrane and poly-Si resistor mounted on a Si substrate (See Figure 5 for top view and cross-sectional designation of a microheater). Starting with a clean, 4-inch, (1 0 0) Si wafer, there is a thermal oxide ( $\text{SiO}_2$ ) layer grown. This  $\text{SiO}_2$  is probably grown under wet oxidation at  $1150^\circ\text{C}$  [2]. Then a layer of silicon rich nitride ( $\text{SiN}_x$ ) is deposited via low pressure chemical vapor deposition (LPCVD) on top of the oxide layer at  $750^\circ\text{C}$  from  $\text{SiH}_4$  and  $\text{NH}_3$  so that the total thickness of both  $\text{SiO}_2$  and  $\text{SiN}_x$  is approximately  $0.7 \mu\text{m}$ . The “x” in this case of  $\text{SiN}_x$  could be 1.2, which is a stoichiometry that has been researched by Rossi in uses within microheaters [8].  $\text{Si}_3\text{N}_4$  is another possible material. The argument for using  $\text{SiN}_{1.2}$  instead of  $\text{Si}_3\text{N}_4$  has to do with residual stresses. The dielectric membrane is thin ( $0.7 \mu\text{m}$ ) and therefore fragile, so any appreciable residual stresses after deposition could cause fracture. It is a good rule of thumb to keep total residual stress under  $0.1 \text{ GPa}$  [8].

In this multilayer dielectric membrane, the  $\text{SiO}_2$  exhibits compressive residual stresses of approximately 0.27 GPa. To balance this, both  $\text{SiN}_{1.2}$  (0.6 GPa) and  $\text{Si}_3\text{N}_4$  (1.2 GPa) have tensile residual stresses, so that when the thicknesses of the two layers are controlled, the overall residual stress is less than 0.1 GPa.  $\text{SiN}_{1.2}$  is favored because it has a smaller, less significant residual stress, which makes balancing the compressive and tensile forces easier. Also,  $\text{Si}_3\text{N}_4$  has shown problems adhering to  $\text{SiO}_2$  [8], which might be a result of the large difference between residual stress magnitudes. This is another argument for the use of  $\text{SiN}_{1.2}$ .

The next step in the fabrication of the microheater is the deposition of 0.5  $\mu\text{m}$  of polycrystalline silicon by LPCVD at 605°C. After using a photoresist in patterning, the resistor takes shape via gas plasma reactive ion etching (RIE) of  $\text{CF}_4$  and  $\text{O}_2$ . Using the same photoresist, a layer of gold is deposited on the substrate, and then the gold pads are realized by the lift-off method. The deposition method for the gold is not discussed, but some possibilities include sputtering or chemical vapor deposition (CVD). There is also no mention of the use of the same photoresist in this step as in the RIE step. It is logical to assume, though, that a photoresist was needed to perform lift-off, and it is also logical to assume an additional photolithography step would have been avoided by reusing the same photoresist.

A square window is opened on the back-side of the wafer through photolithography and gas plasma RIE of  $\text{CF}_4$  and  $\text{O}_2$ . To create the thin membrane on the front of the wafer, the Si substrate is anisotropically etched away, using KOH (no T given), starting at the back-side. The nature of the KOH etch provides a pyramidal etch pit, the size of which can be controlled by the mask size and alignment and the time

allowed for etching. Since there is no etch stop such as a p-n junction, time is the only control on when the etching stops. It is in this pyramidal shaped etch pit, that the microrocket's convergent section is formed. Assuming the photoresist is stripped prior to KOH etching (there was no mention otherwise in Rossi's design), then the rest of the wafer, including the resistor and gold pads, would be exposed to the etchant and therefore be inadvertently damaged in the formation of the convergent. If this were the case, one possible solution would be to change etchants. KOH is the most popular Si etchant for its high etch rates (including relatively high nitride and oxide etch rates), but Tetramethyl Ammonium Hydroxide-Water (TMAHW) has its advantages as well. Although its silicon etch rates are slower, its high selectivity to silicon oxide and silicon nitride along with its ease of use (non-toxic, inexpensive, and abundant in most laboratories) make it a good fit for this application [9] (See Figures 6 and 7 for images of the microheater/convergent).

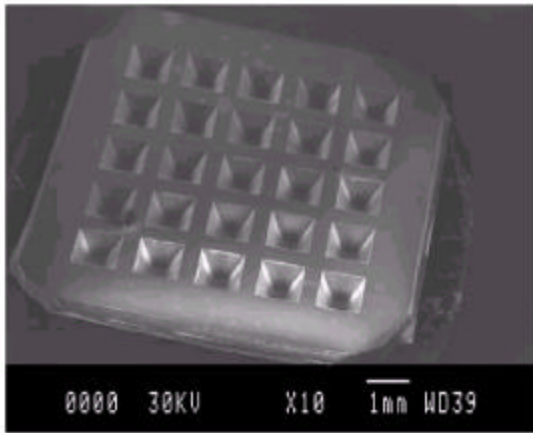


Figure 6 : view from backside of array of Microheaters [6]

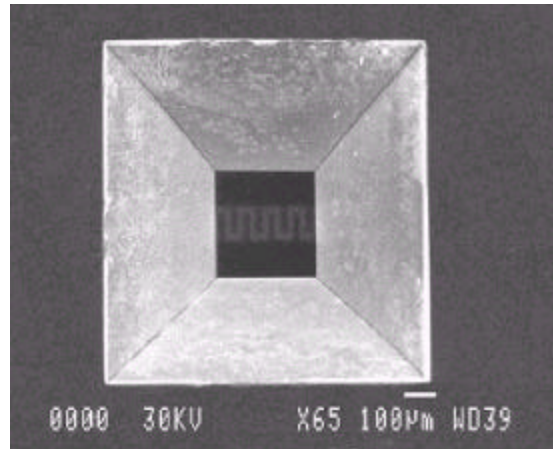


Figure 7: view from backside of single microheater with membrane and resistor visible [6]

### *Propellant Chamber*

The propellant chambers are made using deep reactive ion etching (DRIE) of silicon substrates, with the use of a thick photoresist mask (see Figures 5 and 6 for

images of propellant chambers). It should be noted that there is a discrepancy in the depth of the propellant chamber. In Figure 4, the dimension is given as 1 mm, but in Figure 9, the array of propellant chambers is only 525  $\mu\text{m}$  deep. Silicon wafers come in standard thicknesses, and it could be that there is no way to get a 1mm thick Si wafer. Therefore, Rossi could have used two wafers (525  $\mu\text{m}$  thick), anodically bonded together, to realize the 1mm-long propellant chamber. This is only one possible explanation, as the exact method is not discussed in the article.

The machine used in DRIE is from Surface Technology Systems (STS) with inductively coupled plasma. It is assumed that the Bosch advanced silicon etch (ASE) was utilized, because the etching process is described as including etching and passivation cycles. In ASE, there are active cycles of gas flow ( $\text{SF}_6$ ) for 5-15 seconds, followed by 5-12 seconds of passive gas flow ( $\text{C}_4\text{F}_8$ ). Relatively high etch rates of 1.5-4  $\mu\text{m}/\text{min}$ . have been reported [9], which support the use of this technique for larger depth etching. Also, DRIE is capable of high aspect ratio structures (HARS) as is evident by the reported sidewall angles of  $90^\circ \pm 2^\circ$  [9]. This characteristic is appealing for applications like this propellant chamber, where a vertical wall is needed to meet design specifications.

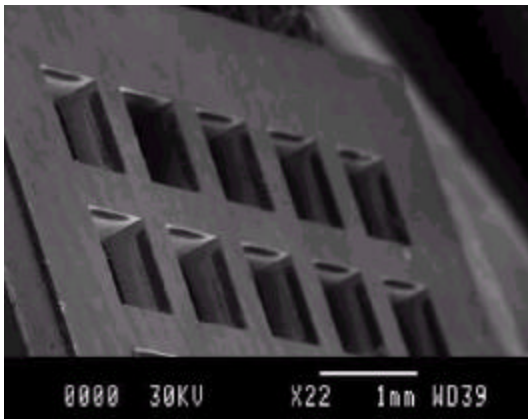


Figure 8: array of propellant chambers [6]

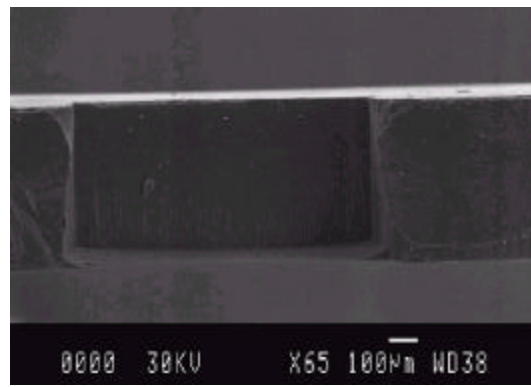


Figure 9: edge on view of cross-sectioned propellant chamber exhibiting unacceptable slope of sidewalls [6]

Even though DRIE is capable of HARS, there are small inconsistencies that get magnified, even over relatively small depths on the order of 1 mm, and become unacceptable. In Rossi's research, propellant chamber etch holes started out with the correct dimensions (1000  $\mu\text{m}$  x 1000  $\mu\text{m}$ ), but by the time they etched through the other side of the wafer (525  $\mu\text{m}$  thick), the dimensions were off by 35  $\mu\text{m}$  per side (see Figure 6). This problem of side walls losing verticality, is due to long etch times, so one possible solution would be to etch from both sides of the wafer. Orientation of photoresist masks would have to be aligned exactly with each other, but this method would decrease the etch time and possibly solve the problem.

Utilizing LIGA would be another possible solution to the verticality problem. Using this process would require realization by the addition of material (lithography) instead of taking material away (etching). For a 400  $\mu\text{m}$  thick structure, the fluctuation in lateral dimensions is only about 0.2  $\mu\text{m}$  [10]. This is a much higher aspect ratio than Rossi is currently obtaining using DRIE. The cost and lack of facilities, however, make this process unappealing for lithography purposes.

Another possibility of using LIGA technology lies in its molding capabilities. The Rossi group has already entertained the possibility of using ceramics instead of silicon for the propellant chamber. They have experimented with micromachining MACOR, a glass ceramic product from Corning, and have also thought about using ceramic injection molding (CIM) to fabricate propellant chambers. In regards to the CIM process, LIGA, with its high aspect ratios, could provide a viable solution for the construction of molds. The only problem is that they are limited in height to a couple of

microns [10]. The high cost of the LIGA process would be counterbalanced by the ability for repeat use of the mold. For lower cost molds, rapid prototyping, which utilizes low viscosity thermoplastic binders or silicon rubber molds, could be another option [11].

### *Divergent*

Although not covered in the report, the fabrication of the diverging part could be assumed to involve standard lithography and anisotropic etching. There may or may not be an oxide layer grown followed by the spin coating of a photoresist. A mask would be used to open a window of specified size and orientation for anisotropic etching. KOH is the most commonly used anisotropic etchant, and the 80° angle of the divergent sidewalls could be achieved with a high-concentration KOH (45 wt%) etch at higher temperatures (80°C) [9].

### *Assembly of Components*

After all components have been fabricated, the propellant chamber and convergent need to be filled with fuel (see Figure 10 for filling device) before the assembly of the components can occur. The fuel is a viscous material, and so the filling procedure has to ensure complete filling of any cavities to prevent air pockets from forming. Therefore, a vacuum must be present during filling. The standard filling procedure involves enclosing the entire filling machine in a chamber where a vacuum can be pulled. The new technology, from NOVATEC SA, used by Rossi involves only a localized vacuum around the gap to be filled. The efficiency and reliability of this system has shown similar results to the old technique while greatly reducing the cost of the process. After filling, the components are assembled with EPO TEK H70E glue,

enabling the microrocket to withstand combustion pressure. The glue is cured at 60°C for 15 hours.

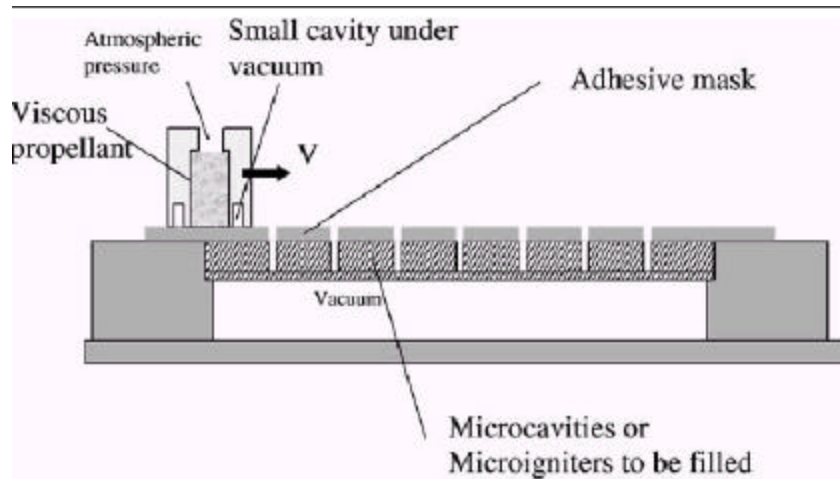


Figure 10: schematic of fuel filling machine and process [6]

## Materials Considerations

### *Propellant Chamber*

It is preferable that the fuel chamber be made of a material with a low thermal conductivity so that less thermal energy from the combustion of the fuel leaks out and more thrust can be obtained from the rocket. Silicon, while amenable to established micromachining processes, may not be the optimal choice in this respect given its moderately high thermal conductivity. On the other hand, ceramic materials can have a thermal conductivity 4 to 10 times less than silicon and can be considered as an alternative material for the construction of the fuel chamber. For current millimeter size scales, chambers can be fabricated by conventional drilling, in this case using the commercial ceramic Macor® (Corning). Table 1 gives a comparison of selected properties of silicon and Macor®. Micromachining the ceramic becomes somewhat of an

issue for smaller size scales, although the possibility of adapting ceramic injection micromolding techniques for this application are promising.

<b>Property</b>	<b>Silicon<sup>1</sup></b>	<b>Macor®<sup>2</sup></b>
Thermal Conductivity	124 W/mK	1.46 W/mK
Thermal Expansion Coefficient 25° – 300°C	$2.49 \times 10^{-6} - 3.61 \times 10^{-6} / ^\circ\text{C}$	$9.3 \times 10^{-6} / ^\circ\text{C}$
Density	2.33 g/cm <sup>3</sup>	2.52 g/cm <sup>3</sup>
Elastic Modulus	112.4 GPa	64 GPa
Temperature Limit	1412°C (melting point)	1000°C

Table 1: Select properties of silicon and Macor® [12,13]

### *Solid Propellant*

Since these rockets are one-time use, stand alone systems that are not meant to be refueled, solid state propellants are preferred for their stability and relatively high energy density. A composite fuel formulated by LaCroix is used and in general consists of a binder material (polybutadiene or glycidyle azide polymer), an oxidizer (NH<sub>4</sub>ClO<sub>4</sub>), and a metallic fuel (Al, Zr, B, Mg). While composite propellants have a relatively low specific heat value and leave metallic particle residue after combustion, they have a greater specific impulse than homogeneous fuels such as nitrocellulose or nitroglycerine and are low vulnerability ammunitions. In particular, the mixtures can be adapted such that the rheological, ballistic and kinetic properties are optimal for the given application.

## **Geometric Considerations**

### *Model*

The propellant is modeled to be burning back from the igniter located at the throat. It is assumed that pressure and temperature are homogeneous in the burning chamber, that the exhaust gas is ideal, that the flow is isentropic, mono-dimensional and quasi-static, and that the effect of pressure on the burn rate is negligible. From this, a self-consistent model can be constructed so that the effect of different design parameters on performance can be evaluated.

### *Chamber-to-Throat Area Ratio*

The chamber-to-throat section ratio ( $A_c/A_t$ ) can easily be modified by changing select fabrication parameters. This ratio is the primary design factor that determines the pressure inside the fuel chamber for a given propellant. Preferably, the pressure should be high enough so that the flow speed at the throat is sonic in order to maximize thrust, but not so high as to destroy the device entirely.

Chamber-to-throat ratios of 60 (chamber diameter 0.85mm, throat diameter 0.108mm) and 16 (chamber diameter 1.00mm, throat diameter 0.25) are fabricated and modeled. The larger rocket can be filled with more fuel and burns slightly longer (0.53sec at external atmospheric pressure) than the smaller rocket (0.42sec at atmospheric). However, the smaller chamber-to-throat ratio of the larger design also means a lower chamber pressure. Results given by the model are summarized in table 2. At atmospheric external pressure, the pressure in the larger chamber is too low to produce sonic flow at the throat, so the thrust delivered is significantly lower than that for the

small rocket. Under an external vacuum (1mbar), both designs achieve sonic flow in the throat and the atmospheric force disappears as well. In this case, both designs perform comparably.

Chamber-to-throat ratio	Steady state burn time (msec)	External Atmospheric (~1bar)			External Vacuum (1mbar)		
		Chamber Pressure (bar)	Thrust force (mN)	Impulse (mN*s)	Chamber Pressure (bar)	Thrust force (mN)	Impulse (mN*s)
16	350	1.2	<1.5	<0.5	0.9	5.0	1.8
60	250	5.0	4.8	1.2	5.0	5.8	1.5

Table 2. – Model results for two different chamber-to-throat ratios

### *Divergent*

The role of the divergent is to accompany the expanding exhaust gas as it exits the throat. If the exhaust section is too large, the gas expands to a lower pressure than the external pressure and a shockwave appears in the divergent. If the section is too small, then the gas exits at a higher pressure and some of the available work energy in the gas is wasted.

While the diverging end is not actually fabricated, it's effect on performance is modeled for the smaller thruster design ( $A_c/A_t = 60$ ). The half-angle of the divergent is fixed at  $8^\circ$ , and the length is varied to study performance in terms of the exit-to-throat area ratio ( $A_e/A_t$ ). At atmospheric external pressure, the optimum diverging length is modeled to be  $50\mu\text{m}$  giving a total thrust of  $1.39\text{mN}\cdot\text{sec}$  (compared to  $1.35\text{mN}\cdot\text{sec}$  for no divergent). As the length increases past optimum, the total thrust rapidly decreases, showing that the divergent is effectively unnecessary due to the relatively low operating

chamber pressure. Under external vacuum however, the optimum exit-to-throat ratio is given as 130, corresponding to a diverging length of 4.0mm and 2.4mN\*sec total thrust.

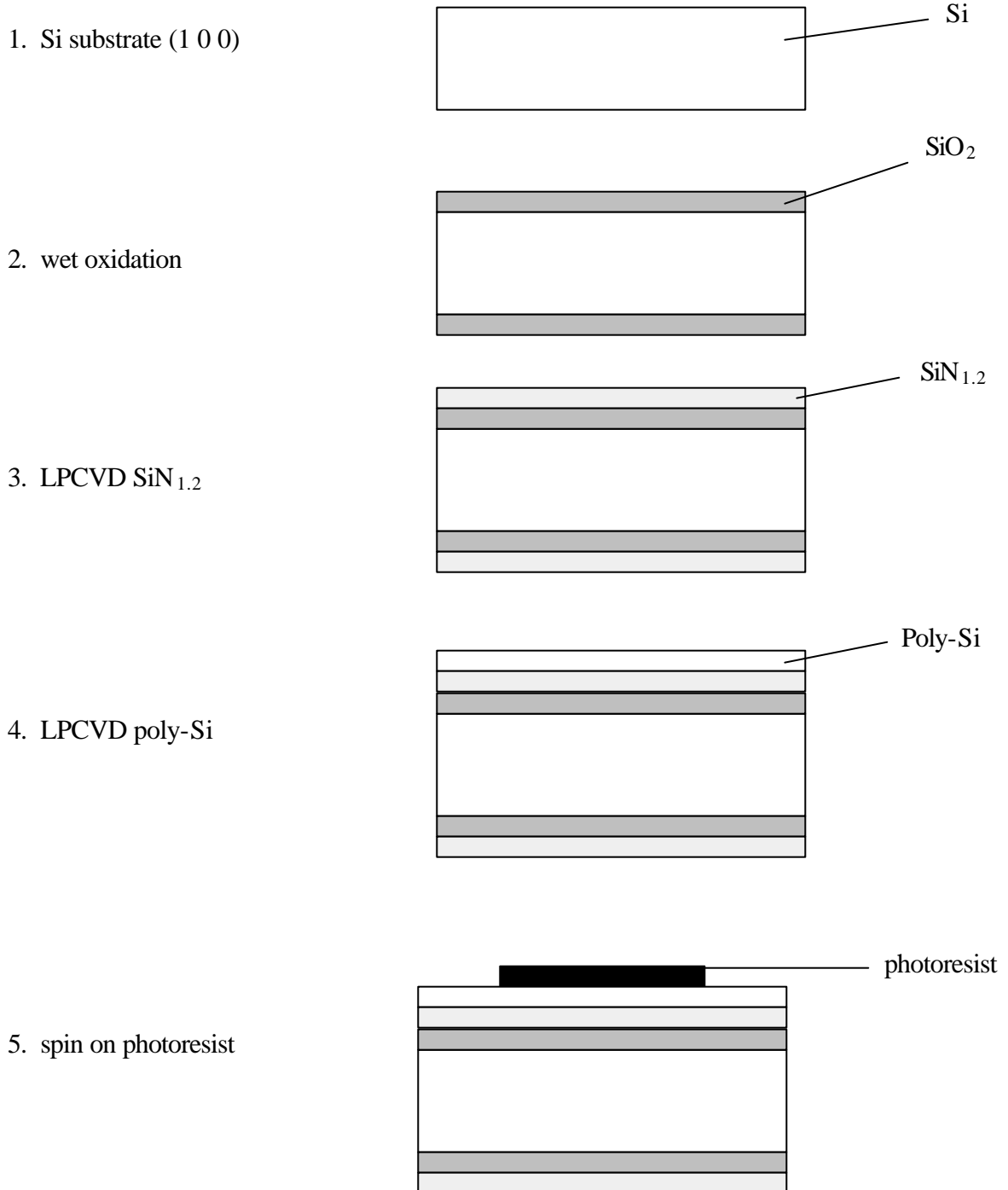
## **Conclusion**

The solid propellant micro-rocket has been developed and shows significant progress towards commercial feasibility. In utilizing various techniques of microfabrication, it is possible to scale a propellant system down to dimensions of technological interest. We have, in this report, analyzed the fabrication process, design considerations and performance results of a solid-propellant micro-rocket system, demonstrating its advantage over other types of micro-rocket devices. In particular, the solid-propelled micro-rocket distinguishes itself by virtue of its relative ease of fabrication, fuel energy density, and efficiency. To be able to apply appropriate techniques of fabrication reliably on such a small scale will inevitably enable the production of such useful devices to flourish. Materials considerations allowing for structural stability and fuel efficiency, including a larger specific impulse for composite propellants than traditional fuels, is one of the leading motivations in continuing this design. Integrating rockets into guidance, positioning, and sensing systems in the end will rest on the reliability of fabrication, a field which continually is evolving and maturing.

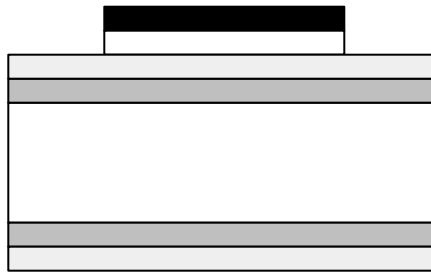
## APPENDIX A: Fabrication Flow Chart

\*\*For more complete description of individual step parameters, see "Fabrication" section

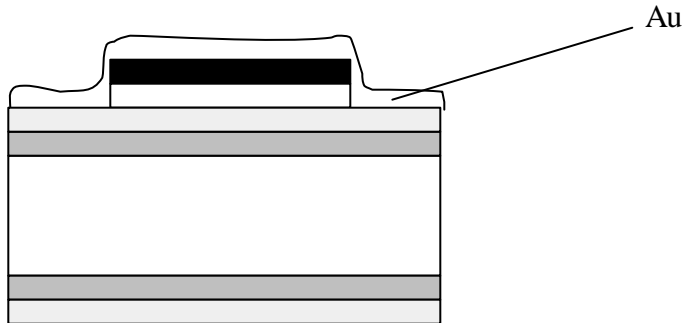
### Microheater/Convergent



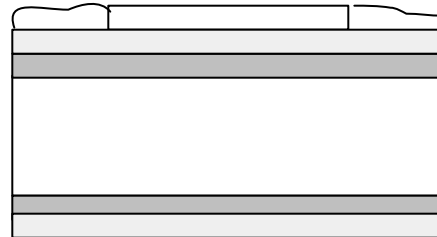
6. gas plasma RIE



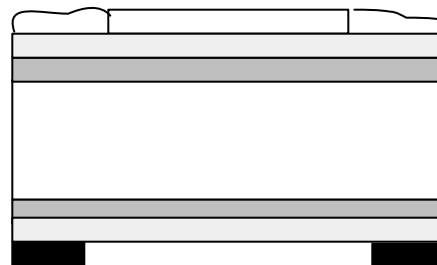
7. Deposition of Au for realization of pads and supply lines



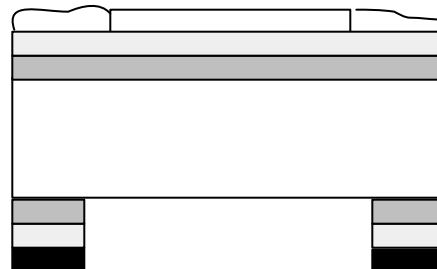
8. Lift-Off



9. spin on photoresist



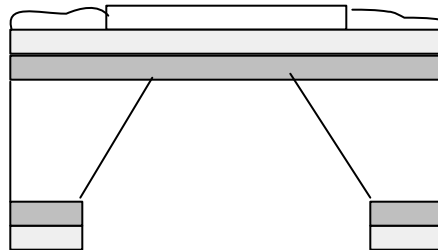
10. gas plasma RIE



11. remove photoresist



12. KOH(TMAHW )  
anisotropic etch

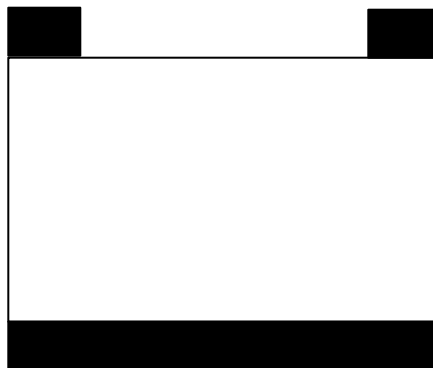


**Propellant Chamber**

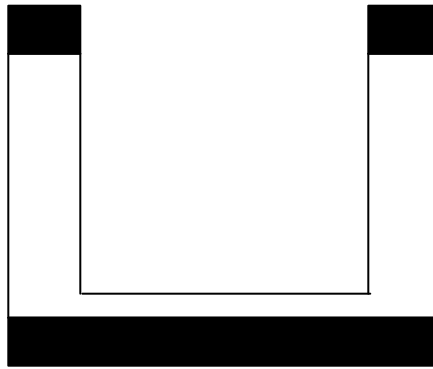
13. Si substrate



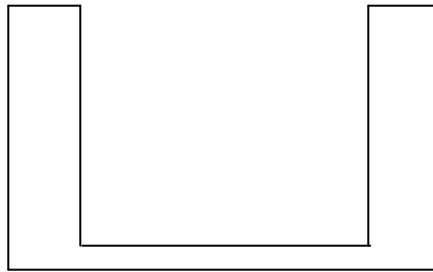
14. spin on photoresist



15. DRIE

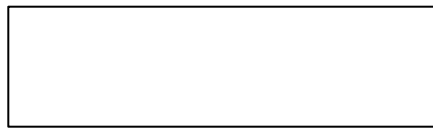


16. remove photoresist

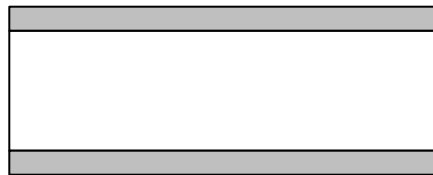


**Divergent**

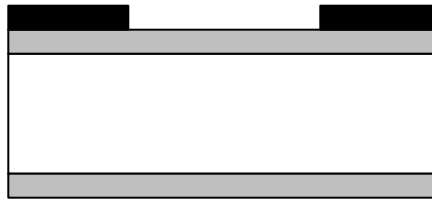
17. Si substrate



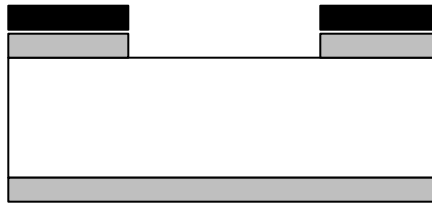
18. grow oxide layer



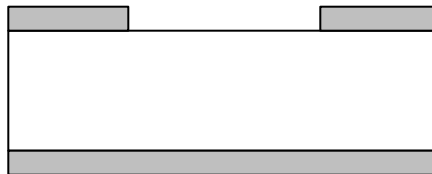
19. pattern photoresist



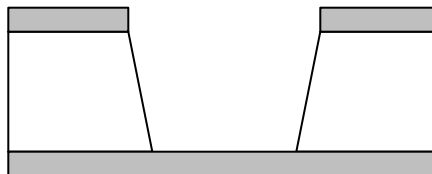
20. gas plasma RIE



21. remove photoresist

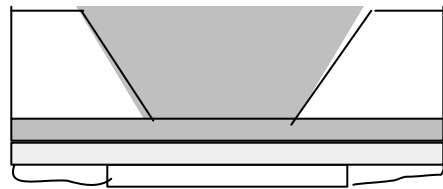
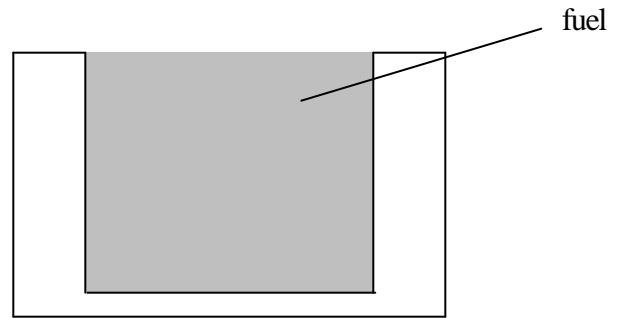


22. KOH anisotropic etch

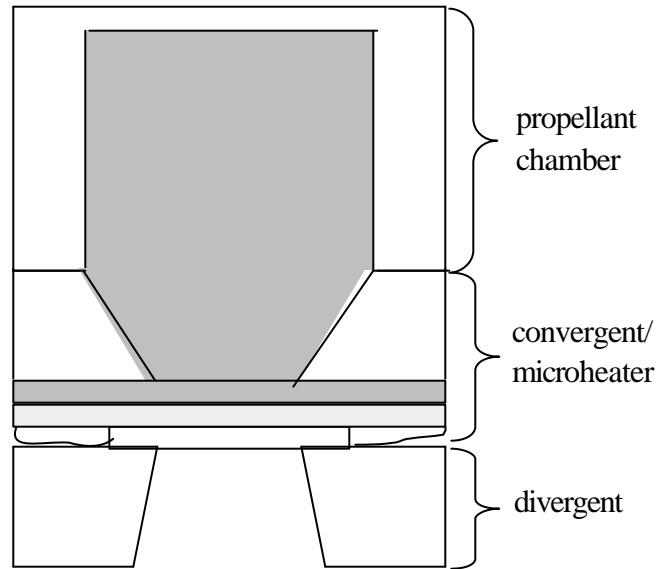


**Assembly of Parts**

23. Fill components with fuel



24. Epoxy bonding of components



## **References**

- [1] 'Smart Dust' K. Pister. <http://robotics.eecs.berkeley.edu/~pister/SmartDust/>
- [2] Livermore, Carl. "Here Come the Microengines." *The Industrial Physicist*. Vol 7, Issue 6. December/January 2001.
- [3] Fréchette, Luc G. et al, *Demonstration of a Microfabricated High-Speed Turbine Supported on Gas Bearings*. Solid-State Sensor and Actuator Workshop, Hilton Head Is., SC. June 4-8, 2000.
- [4] London, A.P. et al. "Microfabrication of a High Pressure Bipropellant Rocket Engine." *Sensors and Actuators: A Physical*. Vol 92. 2001.
- [5] Peles, Y, et al. *Micromachined Rocket Engines*.  
[http://www-mtl.mit.edu/mtlhome/6Res/AR2002/02\\_mems/rocket\\_engines.pdf](http://www-mtl.mit.edu/mtlhome/6Res/AR2002/02_mems/rocket_engines.pdf)
- [6] Rossi, C. et al. "Design, Fabrication and Modeling of Solid Propellant MicroRocket-Application to Micropropulsion." *Sensors and Actuators: A Physical*. Vol 99. 2002.
- [7] "Tiny Propulsion System Targets Future Microsatellites." *Space Daily*.  
<http://www.spacedaily.com/news/nanosat-01b.html>. May 16, 2001.
- [8] Rossi, C., et al., "Realization and performance of thin SiO<sub>2</sub>/ SiN<sub>x</sub> membrane for microheater applications", *Sensors and Actuators A*, vol. 64, (1998) pgs 241-245
- [9] Madou, M., Fundamentals of Microfabrication: The Science of Miniaturization, Second Edition, CRC Press LLC, Boca Raton, FL, (2002) pgs. 104-105, 214-216
- [10] Class Notes from Tuesday, October 22, 2002
- [11] Bauer, W., Knitter, R., "Manufacturing of Ceramic Microcomponents Using Rapid Prototyping Process Chains (RPPC)", *Materials Week 2000*, Sept. 25-28, (2000) Munich
- [12] <http://www.matweb.com/search/SpecificMaterial.asp?bassnum=MESi00>
- [13] <http://www.corning.com/lightingmaterials/products/macor.html>

## **About the Authors**

**Josh Mehling** is a fourth year Mechanical Engineering student at Northwestern University. He is currently completing the requirements for his undergraduate degree in addition to beginning masters level coursework and research in the field of intelligent mechanical systems.

His interest in robotic systems has led to repeat internships with Lockheed Martin Space Operations working at NASA's Johnson Space Center in Houston, Texas. While at the space center's Dexterous Robotics Laboratory, Josh worked primarily on the Robonaut project, NASA's push to develop a next generation robotic astronaut.

**Nik Hrabe** is an undergraduate in his fourth year out of five in the Material Science Department. His concentration within materials science is in nanomaterials. He has been involved in transparent conducting oxide research for the last two years, with his recent efforts focusing in the synthesis of SrCu<sub>2</sub>O<sub>2</sub> for characterization of transport mechanisms and other electrical properties.

Nik is also a part of the co-op program having worked with Dow Corning's Silicon Modified Organics group, and, most recently, Johnson & Johnson's DePuy Orthopaedics in Warsaw, IN, where he is part of the Materials Research Department.

Extracurricular activities include being a former captain and current member of the NU Men's Club Ice Hockey Team, a former Alumni Relations Chairman and current member of the Pi Kappa Alpha fraternity (Gamma Rho colony). Nik enjoys watching movies as well, admiring, in particular, "Buckaroo Banzai: Across the Eight Dimension," "The Last Dragon," and anything with Sandra Bullock in it.

**Arno Merkle** is in his second year of graduate study in the Materials Science and Engineering Department at Northwestern University. He received his undergraduate degree in Physics at Gustavus Adolphus College in St. Peter, MN in 2001. Currently, he is part of the NSF-sponsored Integrated Graduate Research and Traineeship (IGERT) program in Virtual Tribology, which is a common effort amongst several disciplines at Northwestern. His particular areas of interest lie in atomic-scale friction and quasicrystal thin film growth and characterization. Outside of the lab, he spends his time conversing in German and continuing on towards his aspirations of performing his cello on the world's finest concert hall stages.

**Albert Hung** received his B.S. in material science and engineering from M.I.T. in 2001. He is currently in his second year of pursuing a Ph.D. in material science at Northwestern University with Prof. Samuel Stupp. He was awarded a N.D.S.E.G. Fellowship as well as a N.S.F. fellowship for his graduate studies.

Albert's research interests include micropatterning of self-assembling systems and the effect of microscale confinement on material properties and behavior, with a focus on soft condensed matter and polymeric materials.